BIUST Teaching, Research, & Innovation Symposium 2023 (TRDAIS 2023)
Botswana International University of Science and Technology
Palapye, Botswana, 18 - 19 September 2023
ISSN: 2521-2293

GREEN SYNTHESIS OF COPPER OXIDE NANOPARTICLES USING MORULA LEAF EXTRACT AND THEIR APPLICATION IN ADSORPTION OF DYE.

T. Khao[1], *S. Odisitse*[1] *and C. K. Kingóndu*[1]

[1]Chemical and Forensic Sciences, Botswana International University of Science and Technology, Private Bag 16, Palapye, Botswana

ABSTRACT

Morula leaf extract was examined in the synthesis of Copper Oxide (CuO) nanoparticles in this study. The active morula agents are extracted using boiling water followed by hydrothermal treatment with the metal oxide precursors to synthesize the metal oxide nanoparticles. There were no other hazardous substances used apart from water which is considered to be green. X-ray diffraction (XRD) analysis showed that pure and crystalline structures of CuO were fully formed after calcination at 350 °C. CuO was determined by the doublet peak between 200 and 400 cm^{-1} using Raman spectroscopy. Scanning electron microscopy (SEM) and Brunauer–Emmet–Teller (BET) analysis were used to analyze the structural morphology and the adsorptive behaviour of the materials, respectively. Through these two methods, platelets were discovered in CuO and the material was discovered to have larger surface areas of 26.8 m^2/g.

CuO material was then applied in the adsorption of dyes. It was observed that methylene blue (MB) and rhodamine 6G (R6G), adsorb well onto CuO material in an adsorption process. CuO has a maximum adsorptive efficiency of 78 %.

Keywords: Green synthesis, morula leaf extract, adsorption, wastewater

I. INTRODUCTION

Water is one of the most critical resources worldwide, and it is the fundamental support of the existence of life. Therefore, the scarcity of good quality water has detrimental effects on every living creature [1]. Despite this fact, water pollution continues to be a significant problem in our rapidly growing world. This issue stems from the rapid explosion of industries, the global population's exponential growth, and climate change [2]. Rivers, dams, and oceans are daily getting contaminated with dyes, heavy metals, papers, and plastics [3]. Dyes such as methylene blue (MB), rhodamine B (RhB), methyl orange (MO), Congo red (CR) are increasingly being used and are now becoming some of the most important sources of industrial pollutants [4]–[6].

Several methods have been developed by scientists to tackle the dye pollution problem. Various physicochemical and biological methods have been used. These include adsorption, degradation, ion exchange, chemical precipitation, membrane filtration and microbial technologies [7], [8]. Adsorption is popular among these methods due to its simplicity, effectiveness, flexibility, and insensitivity to toxic pollutants. Also attributable to the reversibility of the processes, by using a suitable desorption process, the adsorbent can be reused multiple times [8]–[11].

ISSN: 2521-2293

Transition metal oxides (TMOs) being excellent choice of adsorbents has brought up a great deal of obsession amongst scientists to bring about synthesis methods that are environmentally friendly, cost-effective and easy to employ [12]–[15]. Numerous methods have thus far been developed, and some of them are Sol-gel, Electrospinning, Chemical vapor disposition (CVD), Pyrolysis and Biosynthesis. These methods involve the use of large sums of money, chemicals that are harmful to the environment, are time-consuming, and require high technical skills [16]–[19].

Recent developments in research have brought about the concept of green synthesis. This concept tries to efface the problems brought by the methods mentioned above [15]. Microorganisms, plants, plant extracts, sugars and biopolymers are currently being explored in green synthesis of nanosized TMOs [20], [21]. Plant extracts and other plant parts have gained much more popularity due to the biomass abundance of many plants and their ability to generate nanoparticles of varying size, shape, and stability [22],[23]

The aim of this research was to investigate the use of morula leaves to synthesize CuO as a green and cheaper alternative to already existing methods of synthesis.

II. EXPERIMENTAL

A. *Preparation of Morula leaf extract and characterisation*

The Morula leaves were collected from the tree and rinsed under running water before being dried in a 60 °C oven for 6 h. The leaves were then crushed and stored in a glass bottle for future use.

To obtain the extract, 4 g crushed leaves were cooked in 100 mL distilled water while constantly stirring for 5 mins. The leaves were then filtered, and the new filtrate characterised using contraAA 700 atomic absorption spectroscopy before being used for synthesis.

B. *Synthesis of nanomaterials*

The materials were prepared using a hydrothermal process. 100 mL leaf extract was combined with 20 g of different metal precursors (zinc nitrate, cupric nitrate, and potassium permanganate). After that, the mixture was placed in a hydrothermal reactor and transferred to an oven set at 150 °C. After that, the product was filtered, rinsed, and dried in a 60°C oven overnight.

C. *Characterization of the nanomaterials*

The crystalline structure of the materials was investigated using X-Ray diffractions (XRD) on a Bruker D8 Advance powder diffractometer. A Cu tube X-ray source (λ=1.54056 nm, 40 kV, 40 mA) was employed and the XRD was set at a scan rate of 0.500 sec/step covering 0.02 degrees of 2θ. Spectroscopic studies were performed using the LabRAM HR800 Raman spectrophotometer, which excited the samples with a 532 nm laser.

Morphological analysis of the materials was also done using the JEOL JSM-7500F Field Emission Scanning Electron Microscope (FE-SEM) Equipped with Energy Dispersive X-ray spectroscopy (EDX) which was also employed in further analysis of the materials' elemental composition. Finally, the materials surface area, pore size, and volume were determined using nitrogen at 77 K. Micromeritics Tristar II Brunauer-Emmett-Teller (BET) analyser was employed in this regard

ISSN: 2521-2293

D. Batch equilibrium studies (adsorption)

The impact of variables like contact time and temperature on dye removal from wastewater via adsorption onto metal oxide nanoparticles was investigated. For the investigation, batch adsorption procedures were used. 2 ppm mixtures of methylene and rhodamine dyes were prepared in 250 mL Erlenmeyer flasks. 20 mL of the mixture was then transferred into a beaker and 15 mg of the adsorbent dispersed into the mixture. The mixture was then constantly stirred with a magnetic stirrer until an equilibrium was attained. The supernatant liquids from the centrifuged mixtures were examined with a UV–vis spectrophotometer. The adsorption capacity and dye removal % were calculated using the formulae below:

$$Q_e = \frac{(C_o - C_e)}{W} V \quad (1)$$

$$dye\ removal\ \% = \frac{C_o - C_e}{C_o} \times 100 \quad (2)$$

The initial and equilibrium concentrations (mg/L) are C_0 and C_e, respectively. W is the mass of adsorbent employed (g), and V is the volume of solution (L).

III. Results and discussion

A. Characterization

Synthesis of CuO was initially attempted without the morula leaf extract. Distilled water was the only solvent utilized in the process. Copper Nitrate was mixed with distilled water and the mixture was hydrothermally treated at 150 °C. This reaction resulted in a blue solution without any precipitate as shown in Error! Reference source not found.a below. This shows that the CuO precipitation was aided by the morula leaf extract.

Error! Reference source not found.b depicts the XRD patterns of the CuO materials prepared using the morula leaf extract before and after calcination at temperatures of 250, 300, 325, and 350 °C. CuO was amorphous before calcination. After calcination at 250 °C, peaks began to emerge. Some of the peaks are indicative of CuO at calcination temperatures of 250 and 300 °C, but there are some contaminant peaks as well. Only samples calcined at 325 and 350 °C show XRD peaks, indicative of CuO with no impurities and matches Crystallography Open Database (COD) card no. 1011194. The strongest peaks were found at 34, 38, 49, 54, 59, 61, and 65° corresponding to the lattice planes (110), (111), (202), (020), (202), (202), and (022), respectively.

The particle size was determined using the Debye Scherrer equation. The average particle size of CuO was 10.8 nm after calcination at 350 °C. The sample was subsequently taken for further study using Raman spectroscopy after being calcined at 350 °C.

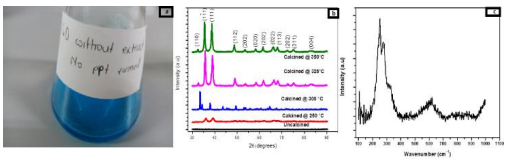

Fig. 1: (a) Optical image of the solution obtained after attempted synthesis of CuO using distilled water instead of morula leaf extract, (b) XRD pattern of CuO synthesized using the morula leaf extract, after calcination at different temperatures, (c) Raman spectrum of CuO synthesized using morula leaf extract and calcined at 350 °C.

The Raman spectra further indicated the formation of CuO during calcination at 350 °C. Nine zone-center optical phonon nodes of CuO with symmetries $4A_u + 5B_u + A_g + 2B_g$ have been reported. Only three of those

ISSN: 2521-2293

A_g and $2B_g$ are Raman active [24]. CuO Raman spectrum in Error! Reference source not found.c exhibits a doublet peak between 200 and 400 cm^{-1} and a singlet peak at 600 cm^{-1}. In the doublet peak, the 1st peak can be assigned to the A_g node and the secondone of the B_g nodes. The peak at 600 cm^{-1} could be attributed to the other B_g node. The peaks correspond to the A_g (296 cm^{-1}), B_g (346 cm^{-1}), and B_g (636 cm^{-1}) modes of bulk CuO crystals respectively and no Cu_2O modes are present [24]. This demonstrates the single-phase property of our CuO nanorods.

B. Morphological analysis

The morphology of the samples was examined using scanning electron microscopy (SEM). **Fig. 1**a-c below represents the SEM images of CuO nanoparticles obtained by calcining at 300, 325 and
350 °C, respectively. The morphology of the material calcined at 300 °C is composed of agglomerated platelet-like structures shape, **Fig. 1**a. At 325 °C, the platelet morphology transformed in thick slabs stacked into microcolumns, **Fig. 1**b. At 350 °C the stacking of the slabs was destroyed due to crystal growth via sintering of slabs, **Fig. 1**c.

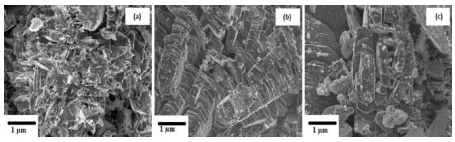

Fig. 1: (a) SEM image of CuO calcined at 300 °C, (b) SEM image of CuO calcined at 325 °C, (c) SEM image of CuO calcined at 350 °C.

Fig. 2a is a representation of the N_2 adsorption-desorption isotherms of the synthesized materials calcined at 300, 325, 350 °C. According to IUPAC classification, all produced materials have typical type V isotherms with an H3-type hysteresis loop. The observed hysteresis loop shape is typical of samples that are mesoporous. The Barret-Joyner-Halenda (BJH) pore size distribution (PSD) profiles are presented in **Fig. 2**b. PSD profiles for the materials calcined at the different temperatures show maxima around 100 Å corresponding 10 nm which falls within the 2–50 nm mesoporous range, meaning no microporosity [25].

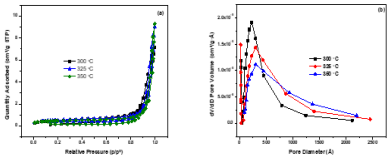

Fig. 2: (a) N_2 adsorption-desorption isotherms (b) Barret-Joyner-Halenda (BJH) pore size distribution curves of CuO materials at 300, 325, and 350 °C.

C. Application

The CuO material was applied as an adsorbent in dye adsorption from water. Figures 7 through 16 show how the material behaves as a dye adsorbent under different condition.

1. Effects of catalyst loading

The influence of adsorbent dose on the efficacy of removing a MB and R6G combination was investigated by adding varying amounts of CuO (0.15, 0.2, 0.25, 0.3, 0.35, and 0.4 mg) while keeping a constant 2 ppm dye concentration. The results are presented in **Fig. 3.** When the CuO dosage was increased from 0.15 to 0.35 mg, the dye adsorption effectiveness increased from 21 to 39% for MB and from 49 to 66% for R6G. The availability of more adsorption sites is responsible for the initial rapid increase in adsorption with increased adsorbent dosage. However, when the CuO dosage was increased beyond 0.35 mg, an equilibrium was reached. The "screening effect," which occurs at higher adsorbent dosage, could be used to explain this phenomenon. It is characterized by the accumulation

ISSN: 2521-2293

of adsorbent particles and a reduction in the distance between adsorbent molecules at the nanoadsorbent surfaces, which results in the formation of a dense screening layer. The dye molecules' binding sites were therefore hidden by the screening layer at the adsorbent's surface [26].

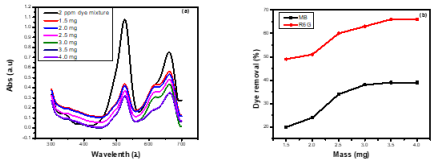

Fig. 3: (a) Effects of adsorbent dosage on adsorption of dye onto CuO, (b) Plot of % dye removal versus amount of adsorbent on adsorption of MB and R6G onto CuO.

2. *Effects of contact time*

Fig. 4 shows the influence of contact time on dye adsorption onto CuO at a starting concentration of 2 ppm. Data was collected at room temperature using a 0.35 mg adsorbent dose and a constant pH of 7.2. According to the graph, the adsorption of both dyes was slow in the first 15 mins. The adsorption rate increased rapidly after 30 mins before it dropped again at 45 mins. Beyond 60 mins, the adsorption rate plateaued. In the first 15 mins of the reactions, the adsorbent had not yet evenly dispersed throughout the dye solution, this caused the slow uptake of the dye molecules. Beyond 15 mins, the adsorbent was event distributed and there was a high number of active sites for dye adsorption, this resulted in increased dye uptake rate. The rate then slowed down and then became constant at 56 and 72% for MB and R6G, respectively, as the active sites of the material were getting filled up and there was no more room to accommodate more dye molecules [26].

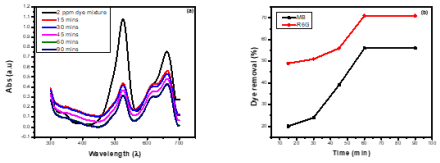

Fig. 4: Effects of contact time on adsorption of dye onto CuO

3. *Effects of temperature*

The impact of temperature on dye adsorption was investigated, and the results presented in Error! Reference source not found.. The temperature ranged from ambient temperature to 90 °C. At 25 °C, CuO adsorption capability was observed to be highest reaching about 56 and 72% for MB and R6G, respectively, at room temperature. The adsorption capacity declined from 56 and 72% to close to 0% when the temperature was increased from room temperature to 90 °C, demonstrating that the process was exothermic. Dye adsorption tends to decrease with increase in temperature as molecules adsorbed earlier tend to desorb from the surface at elevated temperatures. This is caused by the weakening of the attractive forces between the material and the dye molecules at high temperatures [27].

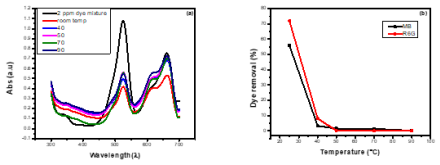

Fig. 6: (a) Effects of temperature on adsorption of a dye mixture onto CuO, (b) Plot of % removal versus temperature on adsorption of MB and R6G onto CuO.

4. *Effects of pH*

Error! Reference source not found. demonstrates the effects of pH on dye adsorption onto CuO. (0.35 mg at room temperature for 1 h). The graph shows that the dye uptake was initially slow from pH 2 to 9. The

ISSN: 2521-2293

adsorption capacity of the methylene blue and rhodamine mixture increased dramatically from pH 9 to 12, reaching 78% for MB and 86% for R6G. It is worth noting that the adsorption efficiency is influenced by the pH of the solution. The active group chemistry and surface charges of CuO changed when the pH was modified [90]. In basic aqueous media, hydroxyl (OH) groups occupy functional binding sites of the CuO material, while protons (H+) occupy functional binding sites of the material in acidic solutions. Between pH 2 and 7, more protons are occupying the hydroxyl vicinities of CuO surfaces. This promotes the initiation of repulsive force (between positive charged dye molecules and the CuO surface), which limits dye binding to some extent and produces a substantial drop in the rate of adsorption [4]. Between 7 and 9, there is an increase in the hydroxyl ions, but it is not yet enough to increase the rate of dye uptake. Beyond pH 9, the OH negative charges on CuO surfaces are widely spread which increases the electrostatic interaction potential between active binding sites and dye species. This resulted in the rapid increase in the dye uptake [28].

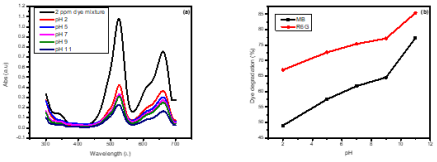

Fig. 7: (a) Effects of pH on adsorption of a dye mixture onto CuO, (b) Plot of % removal versus pH on adsorption of MB and R6G onto CuO.

5. Effects of initial concentration of contaminant

In **Error! Reference source not found.**, the effect of concentration on dye removal using CuO is shown. The results were collected at room temperature with a constant pH of 7.2 and an adsorbent dose of 0.35 mg. The contact time was similarly set at 30 mins. With increasing adsorbate concentration, the amount of dye absorbed (mg/g) was shown to decrease. The blocking action of dye molecules on pores and channels is thought to be the cause of the reduced absorption capacity. The adsorbent sites become totally saturated when the concentration of dye increases without increasing the surface area of the adsorbent, resulting in a decrease in dye removal [22].

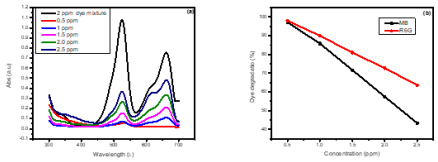

Figure 8: (a) Effects of concentration on adsorption of a dye mixture onto CuO, (b) Plot of % removal versus concentration on adsorption of MB and R6G onto CuO.

V. CONCLUSIONS

CuO possessing a platelets like structure was successfully synthesized using morula leaf extract and this was verified to be the case using XRD and Raman spectroscopy. The surface area of CuO was found to be 26.82 m^2/g which is larger than any previously reported in literature. This demonstrates that the extract was crucial in improving the surface area of the material. The material was then utilized as an adsorbent. Adsorption onto CuO is aided by increasing the adsorbent dose, pH, and contact time.

VI. ACKNOWLEDGMENTS

Authors wish to thank Botswana International University of science and Technology and the department of chemical and forensic sciences for providing instrument facilities to carry out the research work.

ISSN: 2521-2293

IV. REFERENCES

[1] "Botswana Water Sector Policy Brief 2012."

[2] D. Melissa, "Water Pollution: Everything You Need to Know," *Nrdc*, 2018.

[3] P. K. Raul, "CuO nanorods: A potential and efficient adsorbent in water purification," *RSC Adv*, 2014, doi: 10.1039/c4ra04619f.

[4] L. Pereira and M. Alves, "Dyes-environmental impact and remediation," in *Environmental Protection Strategies for Sustainable Development*, 2012, pp. 111–162. doi: 10.1007/978-94-007-1591-2_4.

[5] K. Hunger, *Industrial Dyes: Chemistry, Properties, Applications*. 2003. doi: 10.1021/ja0335418.

[6] D. Gola, "Silver nanoparticles for enhanced dye degradation," *Current Research in Green and Sustainable Chemistry*, vol. 4, Jan. 2021, doi: 10.1016/j.crgsc.2021.100132.

[7] S. Noreen, "ZnO, MgO and FeO adsorption efficiencies for direct sky Blue dye: equilibrium, kinetics and thermodynamics studies," *Journal of Materials Research and Technology*, vol. 9, no. 3, pp. 5881–5893, 2020, doi: https://doi.org/10.1016/j.jmrt.2020.03.115.

[8] J. H. Park, J. J. Wang, Y. Meng, Z. Wei, R. D. DeLaune, and D. C. Seo, "Adsorption/desorption behavior of cationic and anionic dyes by biochars prepared at normal and high pyrolysis temperatures," *Colloids Surf A Physicochem Eng Asp*, vol. 572, pp. 274–282, Jul. 2019, doi: 10.1016/j.colsurfa.2019.04.029.

[9] S. Noreen, "ZnO, CuO and Fe2O3 green synthesis for the adsorptive removal of direct golden yellow dye adsorption: Kinetics, equilibrium and thermodynamics studies," *Zeitschrift fur Physikalische Chemie*, vol. 235, no. 8, pp. 1055–1075, Aug. 2021, doi: 10.1515/zpch-2019-1599.

[10] Y. Kuang, X. Zhang, and S. Zhou, "Adsorption of methylene blue in water onto activated carbon by surfactant modification," *Water (Switzerland)*, vol. 12, no. 2, Feb. 2020, doi: 10.3390/w12020587.

[11] A. S. Elfeky, H. F. Youssef, and A. S. Elzaref, "Adsorption of Dye from Wastewater onto ZnO Nanoparticles-Loaded Zeolite: Kinetic, Thermodynamic and Isotherm Studies," *Zeitschrift fur Physikalische Chemie*, vol. 234, no. 2, pp. 255–278, Feb. 2020, doi: 10.1515/zpch-2018-1342.

[12] P. Tundo., "Synthetic pathways and processes in green chemistry. Introductory overview," 2000. doi: 10.1351/pac200072071207.

[13] S. K. Sharma, H. Demir, S. K. Sharma, and H. Demir, "Principles of Green Chemistry," in *Green Chemistry in Scientific Literature*, 2019. doi: 10.1201/9781003002352-3.

[14] V. Polshettiwar and R. S. Varma, "Green chemistry by nano-catalysis," *Green Chemistry*, 2010, doi: 10.1039/b921171c.

[15] O. O. E. US EPA, "Basics of Green Chemistry," *EPA.GOV*, 2013.

[16] C. Suryanarayana and B. Prabhu, "Synthesis of Nanostructured Materials by Inert-Gas Condensation Methods," in *Nanostructured Materials: Processing, Properties, and Applications: Second Edition*, 2006. doi: 10.1016/B978-081551534-0.50004-X.

[17] T. Guo, M. S. Yao, Y. H. Lin, and C. W. Nan, "A comprehensive review on synthesis methods for transition-metal oxide nanostructures," *CrystEngComm*, 2015, doi: 10.1039/c5ce00034c.

[18] A. Tavakoli, M. Sohrabi, and A. Kargari, "A review of methods for synthesis of nanostructured metals with emphasis on iron compounds," *Chemical Papers*. 2007. doi: 10.2478/s11696-007-0014-7.

[19] C. Dhand, "Methods and strategies for the synthesis of diverse nanoparticles and their applications: A comprehensive overview," *RSC Advances*. 2015. doi: 10.1039/c5ra19388e.

[20] S. Iravani, "Green synthesis of metal nanoparticles using plants," *Green Chemistry*, 2011, doi: 10.1039/c1gc15386b.

[21] M. Ioelovich, "GREEN CHEMISTRY AND TECHNOLOGY OF PLANT BIOMASS," 2018.

[22] H. R. El-Seedi, "Metal nanoparticles fabricated by green chemistry using natural extracts: Biosynthesis, mechanisms, and applications," *RSC Advances*, vol. 9, no. 42. Royal Society of Chemistry, pp. 24539–24559, 2019. doi: 10.1039/c9ra02225b.

[23] S. Lyubchyk, "Integrated Green Chemical Approach to the Medicinal Plant Carpobrotus edulis Processing," *Sci Rep*, vol. 9, no. 1, Dec. 2019, doi: 10.1038/s41598-019-53817-8.

[24] M. Rashad, M. Rüsing, G. Berth, K. Lischka, and A. Pawlis, "CuO and Co3O4 nanoparticles: Synthesis, characterizations, and raman spectroscopy," *J Nanomater*, vol. 2013, 2013, doi: 10.1155/2013/714853.

[25] M. P. Geetha, P. Pratheeksha, and B. K. Subrahmanya, "Development of functionalized CuO nanoparticles for enhancing the adsorption of methylene blue dye," *Cogent Eng*, vol. 7, no. 1, Jan. 2020, doi: 10.1080/23311916.2020.1783102.

ISSN: 2521-2293

[26] N. K. Soliman, "Experimentally and theoretically approaches for disperse red 60 dye adsorption on novel quaternary nanocomposites," *Sci Rep*, vol. 11, no. 1, Dec. 2021, doi: 10.1038/s41598-021-89351-9.

[27] P. Senthil Kumar, "EFFECT OF TEMPERATURE ON THE ADSORPTION OF METHYLENE BLUE DYE ONTO SULFURIC ACID–TREATED ORANGE PEEL," *Chem Eng Commun*, vol. 201, no. 11, pp. 1526–1547, Nov. 2014, doi: 10.1080/00986445.2013.819352.

[28] A. El-Maghraby, A. El-Maghraby, and H. A. el Deeb, "Removal of a basic dye from aqueous solution by adsorption using rice hulls Heba El deeb City of Scientific Researches and Technology Applications (SRTA) Newborg Al-Ara… REMOVAL OF A BASIC DYE FROM AQUEOUS SOLUTION BY ADSORPTION USING RICE HULLS," 2011. [Online]. Available: https://www.researchgate.net/publication/267384112